

# Multiple-Input Multiple-Output Wireless Communication Systems Using Antenna Pattern Diversity

Liang Dong, Hao Ling, and Robert W. Heath, Jr.  
Department of Electrical and Computer Engineering  
The University of Texas, Austin, TX 78712

**Abstract**— Multiple-input multiple-output (MIMO) wireless communication systems employ multiple transmit and multiple receive antennas to obtain significant improvement in channel capacity. However, the capacity is limited by the correlation of sub-channels in non-ideal scattering environments. In this paper, we investigate MIMO systems that use antennas with dissimilar radiation patterns to introduce decorrelation, hence increasing channel capacity. We develop a ray tracing model that takes into account both the propagation channel and the transmit and receive antenna patterns. Using a computational electromagnetic simulator, we show that: (1) MIMO systems that exploit antenna pattern diversity allow for improvement over dual-polarized antenna systems; (2) The capacity increase of such MIMO systems depends on the characteristics of the scattering environment.

## I. INTRODUCTION

Multiple-input multiple-output (MIMO) wireless communication is one of the most promising technologies for improving the spectrum efficiency of wireless communication systems. It is well known that the use of MIMO antenna systems allows the channel capacity to scale in proportion to the minimum of the number of transmit and receive antennas in uncorrelated Rayleigh fading channels [1], [2]. Of course, real channels do not satisfy these ideal assumptions, thus recent work has focused on measuring and characterizing real MIMO propagation channels [3]. In parallel, work is continuing on efficient space-time coding strategies that achieve the benefits of MIMO communication [4], [5]. However, thus far there has been little work on one of the most important aspects of MIMO communication systems – the antennas that are used at both the transmitter and receiver.

The correlation between sub-channels of the matrix channel limits the MIMO channel capacity considerably [6], [7]. One way to reduce correlation is to use antennas with different polarizations and radiation patterns [8], [9]. Recent results on polarization diversity show that up to six degrees of freedom are available in the polarization channel of a rich scattering environment, thus the channel capacity can be increased dramatically [10]. However, the sub-channels created by antenna polarization diversity are not completely decorrelated in a real environment, such that the effective degrees of freedom are much less than six, therefore the capacity increase is limited.

In this paper, we investigated the impact of antenna pattern and polarization on MIMO communication channels. We spe-

cialize our results to the case where the antennas are collocated and thus only pattern and polarization, but not antenna spacing, are the parameters of the spatial signatures. This is important for mobile applications where space is extremely limited [11]. First we analyze MIMO channel capacity under correlated fading. The MIMO channel is decoupled into sub-channels to quantify the effect of channel correlation. Secondly, we introduce a general channel model that shows how pattern diversity is the natural generalization of polarization diversity. We describe how orthogonality between patterns decorrelates the signals in highly scattering environments, hence reducing the capacity loss due to channel correlation. Finally, using an electromagnetic ray-tracing simulator, we show that the increase of channel capacity is determined by the selection of antennas of different patterns, and by various propagation environments.

This paper is organized as follows. In Section II, we introduce the mutual information and the channel capacity of the MIMO wireless system, and discuss the correlation between sub-channels. In Section III, the proposed MIMO system that exploits antenna pattern diversity is described, and pattern diversity is expressed in the channel transfer matrix. Section IV demonstrates the capacity increase obtained through antenna pattern diversity via a ray-tracing simulator. Finally, conclusions are drawn in Section V.

## II. MIMO CHANNEL CAPACITY UNDER CORRELATED FADING

Consider a narrowband MIMO wireless system with  $n_T$  transmit antennas and  $n_R$  receive antennas. The induced voltages at the receive antennas are related to the impressed voltages at the transmit antennas as

$$\mathbf{v}^{(R)} = \mathbf{A}\mathbf{H}\mathbf{v}^{(T)} + \mathbf{n} \quad (1)$$

where  $\mathbf{v}^{(R)} = [v_1^{(R)} v_2^{(R)} \dots v_{n_R}^{(R)}]^T$  are the voltages at the receive antennas,  $\mathbf{v}^{(T)} = [v_1^{(T)} v_2^{(T)} \dots v_{n_T}^{(T)}]^T$  are the voltages at the transmit antennas.  $\mathbf{H}$  is the normalized channel transfer matrix modeling the small-scale fading process,  $A^2$  encompasses the (spatially local-averaged) large-scale path loss and shadowing, and  $\mathbf{n}$  is the additive white Gaussian noise (AWGN) vector. If we assume that the channel state information (CSI) is completely known by the receiver but not by the transmitter, the transmitted signal vector is composed of  $n_T$  statistically independent Gaussian components with equal power. For a narrowband MIMO channel with uniform power allocation constraint,

the mutual information between the transmitter and the receiver is given by [2]

$$M(\mathbf{H}) = \log_2 \left[ \det \left( \mathbf{I}_{n_R} + \frac{\rho}{n_T} \mathbf{H}\mathbf{H}^\dagger \right) \right] \quad (2)$$

where  $\rho$  is the average signal-to-noise-ratio (SNR) at each receive antenna,  $\dagger$  denotes conjugate transpose. The ergodic channel capacity  $C$  is the expectation of  $M(\mathbf{H})$  taken over the probability distribution of  $\mathbf{H}$ . We will assume  $n_T = n_R = n$  throughout the rest of the paper.

Suppose the communication is carried out using bursts (packets). The burst duration is assumed to be short enough such that the channel can be regarded as essentially fixed during a burst, but long enough that the standard information-theoretic assumption of infinitely long code block lengths can be used. In this quasi-static scenario, it is meaningful to associate the ‘‘instantaneous channel capacity’’ with the mutual information given a realization of the channel matrix  $\mathbf{H}$ . From (2), the mutual information can be further expressed as

$$M(\mathbf{H}) = \sum_{i=1}^n \log_2 \left( 1 + \frac{\rho}{n} \lambda_i \right) \quad (3)$$

where  $\{\lambda_i\}$  are the eigenvalues of  $\mathbf{H}\mathbf{H}^\dagger$ . At high SNR, the mutual information can be approximated by

$$M(\mathbf{H}) \approx \sum_{i=1}^{\text{rank}(\mathbf{H})} \log_2 \left( \frac{\rho}{n} \lambda_i \right) \quad (4)$$

Since  $\lambda_i \leq n$  for a normalized  $\mathbf{H}$ , an upper bound of the mutual information (at high SNR) can be derived as [10]

$$M(\mathbf{H}) \leq \text{rank}(\mathbf{H}) \log_2 \rho \quad (5)$$

The equality is achieved when a total of  $\text{rank}(\mathbf{H})$  sub-channels are uncorrelated. However, complete decorrelation is hard to achieve in a practical scattering environment.

In order to quantify the effect of channel correlation, the MIMO channel is decoupled into  $n$  single-input single-output (SISO) sub-channels. Performing the singular value decomposition of the channel matrix  $\mathbf{H}$  as  $\mathbf{H} = \mathbf{U}\mathbf{\Sigma}\mathbf{V}$ , we can rewrite the input-output relationship as

$$\mathbf{y} = \mathbf{\Sigma}\mathbf{x} + \mathbf{u} \quad (6)$$

where,  $\mathbf{y} = \mathbf{U}^\dagger \mathbf{v}^{(R)}$ ,  $\mathbf{x} = \mathbf{A}\mathbf{V}\mathbf{v}^{(T)}$ , and  $\mathbf{u} = \mathbf{U}^\dagger \mathbf{n}$ . Because  $\mathbf{\Sigma}$  is a diagonal matrix, the MIMO channel is transformed into  $n$  SISO sub-channels with gains  $\sigma_1^2, \sigma_2^2, \dots, \sigma_n^2$ , where  $\{\sigma_i\}$  are the diagonal entries of  $\mathbf{\Sigma}$ . The mutual information of the MIMO channel is the sum of the mutual information of the  $n$  sub-channels [6],

$$M(\mathbf{H}) = \sum_{i=1}^n \log_2 \left( 1 + \frac{\rho}{n} \sigma_i^2 \right) \quad (7)$$

where we assume uniform transmitted power allocation on the transmit antennas. This is exactly the mutual information of MIMO channel expressed in (3), with  $\sigma_i^2 = \lambda_i$  being the eigenvalues of  $\mathbf{H}\mathbf{H}^\dagger$ . The channel capacity is determined by the

values of the eigenvalues. When a sub-channel is correlated with another one, the corresponding eigenvalue becomes small, which results in a sub-channel with small gain. From (7) we see that the correlated sub-channel contributes little to the total mutual information.

The decorrelation of sub-channels is conventionally provided by spatial diversity, that is, using spatially separated multiple antennas at the transceivers such that each transmitter-receiver pair experiences a different fading channel. With insufficient spacing of local antennas, however, strong correlation can be exhibited between sub-channels, and consequently the MIMO channel capacity is reduced considerably.

### III. ANTENNA PATTERN DIVERSITY IN MIMO COMMUNICATION

To introduce sub-channel decorrelation to the MIMO system which has insufficient antenna spacing, we propose a transceiver array which is composed of antennas with appropriate dissimilarity in radiation patterns, and allow the antenna pattern diversity to be expressed in the channel transfer matrix. The antenna pattern diversity can be exploited in conjunction with spatial diversity to achieve better channel performance in implementation. However, only pattern diversity is addressed in this context for a clear demonstration.

Suppose the transmit antennas are collocated but have different radiation patterns. The receive antennas are also collocated, each of which has a radiation pattern the same as one of the transmit antennas. For a narrowband channel at fixed carrier frequency  $f_c = c/\lambda$ , the channel transfer matrix  $\mathbf{G} = \mathbf{A}\mathbf{H}$ , where  $\mathbf{A}$  is defined as before,  $\mathbf{H}$  is the normalized channel transfer matrix modeling both the multipath fading process and the antenna pattern diversity. By ray-tracing [12] from the transmit antenna to the receive antenna, the voltage on the  $i^{\text{th}}$  receive antenna excited by the transmission of the  $k^{\text{th}}$  transmit antenna is [13]

$$v_{i,k}^{(R)} = \beta \sum_{m=1}^M \mathbf{E}_k^m \cdot \mathbf{F}_i(\theta_m^{(R)}, \phi_m^{(R)}) \quad (8)$$

where  $\beta$  is a proportionality constant (assume  $\beta = 1$ ),  $M$  is the number of multipaths in the link,  $\mathbf{F}_i(\theta_m^{(R)}, \phi_m^{(R)})$  is the  $i^{\text{th}}$  receive antenna pattern,  $(\theta_m^{(R)}, \phi_m^{(R)})$  is the receiving angle of each ray, and  $\mathbf{E}_k^m$  is the incident field of the  $m^{\text{th}}$  multipath at the receiver. We have

$$\mathbf{E}_k^m = \frac{e^{-jk_0 l_m}}{l_m} \mathbf{f}_{m,k} \left( \mathbf{F}_k(\theta_m^{(T)}, \phi_m^{(T)}) \right) v_k^{(T)} \quad (9)$$

where  $k_0 = 2\pi/\lambda$ ,  $l_m$  is the path length of the  $m^{\text{th}}$  multipath,  $\mathbf{f}_{m,k}(\cdot)$  is the functional of reflection and diffraction of the  $m^{\text{th}}$  multipath, and  $\mathbf{F}_k(\theta_m^{(T)}, \phi_m^{(T)})$  is the  $k^{\text{th}}$  transmit antenna pattern,  $(\theta_m^{(T)}, \phi_m^{(T)})$  the transmitting angle. Therefore  $\mathbf{G}$  has complex scalar entries as

$$G_{i,k} = \sum_{m=1}^M \frac{e^{-jk_0 l_m}}{l_m} \mathbf{f}_{m,k} \left( \mathbf{F}_k(\theta_m^{(T)}, \phi_m^{(T)}) \right) \cdot \mathbf{F}_i(\theta_m^{(R)}, \phi_m^{(R)}) \quad (10)$$

And  $\mathbf{G}$  can be expressed as

$$\mathbf{G} = \sum_{m=1}^M \frac{e^{-jk_0 l_m}}{l_m} \tilde{\mathbf{G}}_m \quad (11)$$

where

$$\tilde{\mathbf{G}}_{m,i,k} = \mathbf{f}_{m,k} \left( \mathbf{F}_k(\theta_m^{(T)}, \phi_m^{(T)}) \right) \cdot \mathbf{F}_i(\theta_m^{(R)}, \phi_m^{(R)}) \quad (12)$$

Because the transmit antennas and the receiver antennas are collocated, the difference in path length and phase of the rays travelling between any transmitter-receiver pairs can be neglected. The difference of the entries of  $\mathbf{G}$  is solely caused by the antenna pattern diversity implied in  $\tilde{\mathbf{G}}_m$ .

One observation is that using the dual-polarized transmitter-receiver pair where two linear dipoles with equal gain are orthogonally collocated at each end, the two sub-channels are almost uncorrelated with the presence of a strong line-of-sight (LOS) multipath component. The relatively large gains  $\sigma_1^2$  and  $\sigma_2^2$  of the sub-channels are provided by the quasi-orthogonal structure of  $\mathbf{H}$ , and the mutual information reaches its maximum among normalized  $2 \times 2$  channel realizations. However, the upper bound of mutual information (5) introduced in [10] is loose in a MIMO system using pattern diversity with a large number of transmitter-receiver pairs. As we will see in the simulation, the mutual information provided by some sub-channels are nearly zero. Although the rank of  $\mathbf{H}$  is guaranteed, the corresponding eigenvalues of  $\mathbf{H}\mathbf{H}^\dagger$  are small compared to the dominant ones, which is a direct result of severe correlation of the sub-channels.

In order to achieve uncorrelated sub-channels, the goal of antenna design is to make the incident fields of the transmission from one antenna align with the radiation pattern of the desired receive antenna, while being orthogonal to the patterns of other receive antennas. However, in the real electromagnetic world, the sub-channels, which are characterized by the summation of the dot products in (10), can not be completely decorrelated.

#### IV. SIMULATIONS

The ergodic channel capacity can be calculated given the distribution of the eigenvalues of  $\mathbf{H}\mathbf{H}^\dagger$ . However, for a general covariance of fading and pattern diversity and a finite dimensionality, the distribution of eigenvalues can be very difficult to compute. In this section, the ‘‘instantaneous channel capacity’’, that is, the mutual information between the transmitter and the receiver, is studied via numerical computation using an electromagnetic ray tracer, FASANT [14]. It is a deterministic ray tracing technique based on geometric optics and the uniform theory of diffraction.

A street lattice in Fig. 1 is simulated as the geometry input of FASANT. The size of each building block is  $(10 \times 10 \times 10) m^3$ , and the street width is 10 m. The material properties of the building walls and the ground are: relative permittivity  $\epsilon = 2.0$ , relative permeability  $\mu = 1.0$ , and conductivity  $\sigma = 0.08$ . There are two transmission points  $T_1 : (20, 20, 5)m$  and  $T_2 : (24, 10, 5)m$ , where  $T_1$  is in the middle of a street crossing. The receiver can move along two streets shown as the tracks  $R_1$  and  $R_2$ .

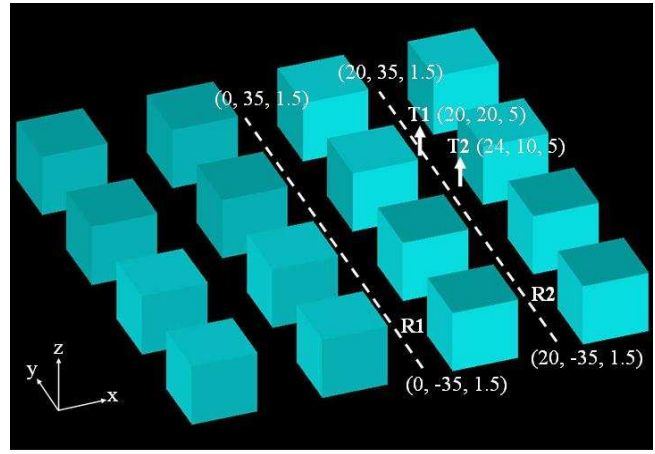


Fig. 1. Street lattice with transmitter positions  $T_1$  and  $T_2$ , and receiver moving tracks  $R_1$  and  $R_2$ .

The infinitesimal electric-dipole of electric source  $\mathbf{J}$  or current-loop of magnetic source  $\mathbf{M}$  is used as the transmit and receive antenna element. At each end of the communication link, two orthogonally placed electric-dipoles with their feed points collocated form a  $2 \times 2$  MIMO system. Three such orthogonally placed electric-dipoles form a  $3 \times 3$  MIMO system, and another three orthogonally placed current-loops, which are referred to as magnetic-dipoles, collocated with the  $3 \times 3$  electric-dipoles form a  $6 \times 6$  MIMO systems. The radiation pattern of the electric-dipole with vertical  $\mathbf{J}$  in the spherical coordinate system is  $\mathbf{E} = \sin(\theta)\hat{\mathbf{a}}_\theta$ , and the radiation pattern of the magnetic-dipole with vertical  $\mathbf{M}$  is  $\mathbf{E} = -\sin(\theta)\hat{\mathbf{a}}_\phi$ . The carrier frequency is 1.8 GHz, that is, a carrier wavelength of 0.167 m.

Given the geometry input with material properties, transmitter and receiver positions, and transmit antenna patterns, the ray tracer FASANT gives outputs such as direction of arrival (DOA), path length and field strength of each multipath arriving the receiver.

##### A. Case 1

In case 1, the transmit antenna array is located at  $T_1$ , and the receive antenna array moves along 4 tracks  $(-1, -35, 3) \rightarrow (-1, 35, 3)$ ,  $(1, -35, 3) \rightarrow (1, 35, 3)$ ,  $(-1, -35, 1) \rightarrow (-1, 35, 1)$ , and  $(1, -35, 1) \rightarrow (1, 35, 1)$ , which are on the same street surrounding track  $R_1 : (0, -35, 1.5) \rightarrow (0, 35, 1.5)$ . Therefore, as the receiver changes its position, it experiences both line-of-sight (LOS) and non-line-of-sight (NLOS) channels.

Fig. 2 shows the eigenvalues of normalized  $\mathbf{H}\mathbf{H}^\dagger$  when the receiver changes its position along each track. Each of the transmit and receive antenna arrays is composed of three electric-dipoles orthogonally placed along  $x$ ,  $y$ ,  $z$  axes of the Cartesian coordinate system and three such orthogonally placed magnetic-dipoles. Therefore, every  $\mathbf{H}$  along the tracks is a realization of the  $6 \times 6$  MIMO channel. As shown in the figure, there are two dominant eigenvalues of  $\mathbf{H}\mathbf{H}^\dagger$  of each realization of the channel, the next two are about 20 dB down, and the weakest two are about 40 dB down the dominant ones. The drop of weaker eigenvalues, especially in the LOS region from

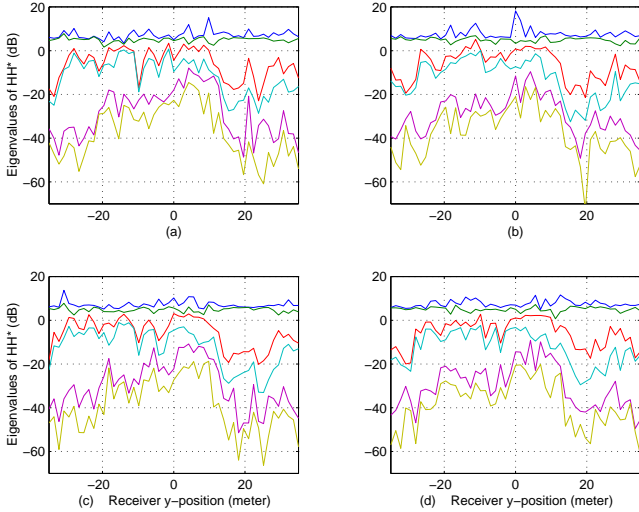


Fig. 2. Eigenvalues of normalized  $\mathbf{H}\mathbf{H}^\dagger$  of the  $6 \times 6$  MIMO channel in Case 1. The transmitter is located at  $T_1$ , and the receiver moves along 4 tracks as: (a)  $(-1, -35, 3) \rightarrow (-1, 35, 3)$ , (b)  $(1, -35, 3) \rightarrow (1, 35, 3)$ , (c)  $(-1, -35, 1) \rightarrow (-1, 35, 1)$ , (d)  $(1, -35, 1) \rightarrow (1, 35, 1)$ .

$y = 13.33$  m to  $y = 26.67$  m, reveals strong correlations between the sub-channels.

Fig. 3 compares the local-averaged mutual information of the  $6 \times 6$  MIMO system with that of the  $2 \times 2$  and  $3 \times 3$  MIMO systems. In the  $2 \times 2$  MIMO system, each of the transmit and receive antenna arrays is composed of two electric-dipoles orthogonally placed along  $y$  and  $z$  axes, such that in the LOS region, the system is similar to a conventional dual-polarized communication system. In the  $3 \times 3$  MIMO system, the array is composed of three electric-dipoles orthogonally placed along  $x$ ,  $y$  and  $z$  axes. The average receive SNR is 20 dB. The figure shows the increase of mutual information of the  $6 \times 6$  and  $3 \times 3$  MIMO systems that use collocated antennas exploiting pattern diversity, over the mutual information of the dual-polarized antenna system as the  $2 \times 2$  MIMO case. The antenna pattern diversity is provided by the scattering environment, as a result, the MIMO channel that exploits antenna pattern diversity in the LOS region has less capacity increase as shown in the figure.

Fig. 4 shows the ratios of mutual information of systems of different numbers of dimension as above. Comparing mutual information of the  $6 \times 6$  system with that of the  $2 \times 2$  system, we find that the “instantaneous capacity” in any position of the scattering environment is not ideally tripled, contrast to what was claimed in [10]. This result is expected from the eigenvalue plot of Fig. 2, because of the non-negligible correlation between sub-channels. Besides two dominant sub-channels as in a dual-polarized system, additional sub-channels of a system with multiple collocated antennas at transmitter and receiver are correlated in a practical scattering environment. The electrical components and the magnetic components of the field are also highly correlated.

### B. Case 2

In case 2, the transmit antenna array is located at  $T_2$ , and the receive antenna array moves along the LOS street  $R_2$  :

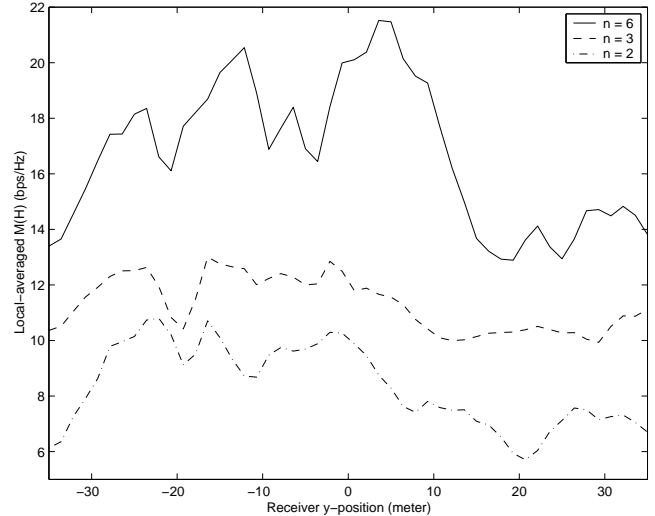


Fig. 3. Mutual information of the  $2 \times 2$ ,  $3 \times 3$  and  $6 \times 6$  MIMO channels in Case 1, averaged over neighboring 8 receiving positions. The LOS region is  $y \in [13.33, 26.67]$  m. Average receive SNR = 20 dB.

$(20, -35, 1.5) \rightarrow (20, 35, 1.5)$ , and the (almost) NLOS street  $R_1 : (0, -35, 1.5) \rightarrow (0, 35, 1.5)$ .

Fig. 5 shows the eigenvalues of normalized  $\mathbf{H}\mathbf{H}^\dagger$  of the  $6 \times 6$  MIMO system, where each of the transmitter and receiver antenna arrays has three electric-dipoles orthogonally placed along  $x$ ,  $y$ ,  $z$  axes, collocated with three such orthogonally placed magnetic-dipoles. Fig. 5(a) shows the eigenvalues of channel realizations when the receiver changes its position along  $R_2$ , the LOS region. Fig. 5(b) shows the eigenvalues of channel realizations when the receiver changes its position along  $R_1$ , the NLOS region. The better decorrelation of sub-channels in a rich scattering environment (NLOS region) is revealed as the increase in value of the smaller eigenvalues.

Fig. 6 compares the complementary cumulative distribution functions (CCDF) of instantaneous channel capacities of the  $2 \times 2$ ,  $3 \times 3$  and  $6 \times 6$  MIMO systems, where the receiver changes position along the LOS and NLOS streets. For the  $2 \times 2$  MIMO system, the transceiver antenna array is composed of two collocated electric-dipoles along  $x$  and  $z$  axes, which forms a dual-polarized system in the LOS region. The  $3 \times 3$  MIMO system has three collocated electric-dipoles at the transceiver along  $x$ ,  $y$  and  $z$  axes. The average receive SNR is 20 dB. As shown in the figure, the large increase in channel capacity of a MIMO system that exploits antenna pattern diversity, referring to a dual-polarized MIMO system, is more likely to occur in a rich-scattering environment (NLOS region).

## V. CONCLUSION

A MIMO wireless system that exploits antenna pattern diversity has been presented. Although the antennas are collocated at the transmitter and receiver, with appropriate dissimilarity in antenna pattern, the system offers large channel capacity promised by the MIMO architecture. The MIMO system with multiple collocated transmit and receive antennas can achieve capacity increase over the dual-polarized system. However, in a practical scattering environment, the capacity increase

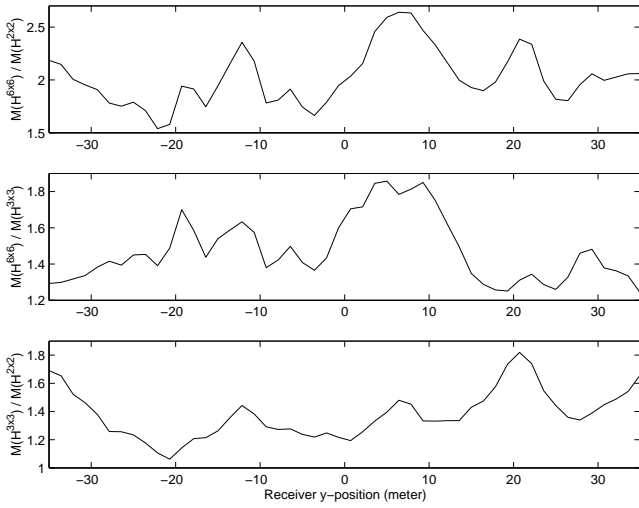


Fig. 4. Ratios of mutual information of  $6 \times 6$  to  $2 \times 2$ ,  $6 \times 6$  to  $3 \times 3$ , and  $3 \times 3$  to  $2 \times 2$  MIMO systems in Case 1.

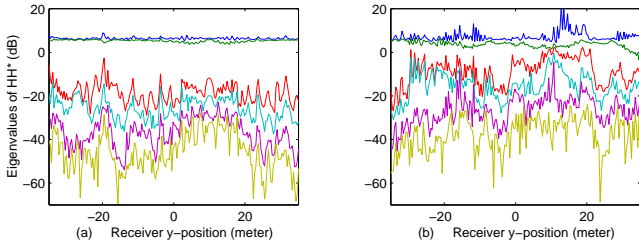


Fig. 5. Eigenvalues of normalized  $\mathbf{H}\mathbf{H}^H$  of the  $6 \times 6$  MIMO channel in Case 2. The transmitter is located at  $T_2$ , and the receiver moves along 2 tracks as: (a)  $R_2$  LOS street. (b)  $R_1$  NLOS street.

is limited due to correlation between sub-channels. The MIMO channel capacity is affected not only by the antenna pattern selection, but by the characteristics of the scattering environment as well.

## REFERENCES

- [1] A. Paulraj and T. Kailath, "U.S. pattern No. 5345599: Increasing capacity in wireless broadcast systems using distributed transmission/directional reception (DTDR)," Sept. 1994.
- [2] G. J. Foschini and M. J. Gans, "On limits of wireless communications in a fading environment when using multiple antennas," *Wireless Personal Commun.*, vol. 6, no. 3, pp. 311–335, Mar. 1998.
- [3] A. F. Molisch, M. Steinbauer, M. Toeltsch, E. Bonek, and R. S. Thomä, "Capacity of MIMO systems based on measured wireless channels," *IEEE J. Select. Areas Commun.*, vol. 20, no. 3, pp. 561–569, Apr. 2002.
- [4] V. Tarokh, N. Seshadri, and A. R. Calderbank, "Space-time codes for high data rate wireless communication: performance criterion and code construction," *IEEE Trans. Inform. Theory*, vol. 44, no. 2, pp. 744–765, Mar. 1998.
- [5] V. Tarokh, H. Jafarkhani, and A. R. Calderbank, "Space-time block codes from orthogonal designs," *IEEE Trans. Inform. Theory*, vol. 45, no. 5, pp. 1456–1467, July 1999.
- [6] D.-S. Shiu, G. J. Foschini, M. J. Gans, and J. M. Kahn, "Fading correlation and its effect on the capacity of multielement antenna systems," *IEEE Trans. Commun.*, vol. 48, no. 3, pp. 502–513, Mar. 2000.
- [7] I. E. Telatar and D. N. C. Tse, "Capacity and mutual information of wideband multipath fading channels," *IEEE Trans. Information Theory*, vol. 46, no. 4, pp. 1384–1400, July 2000.
- [8] B. Lindmark, S. Lundgren, J. R. Sanford, and C. Bechman, "Dual-polarized array for signal-processing applications in wireless communications," *IEEE Trans. Antennas Propagat.*, vol. 46, no. 6, pp. 758–763, June 1998.

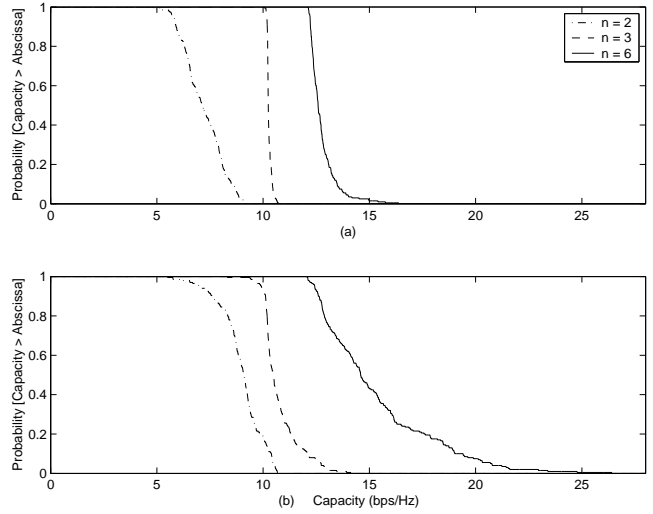


Fig. 6. CCDFs of instantaneous capacities of the  $2 \times 2$ ,  $3 \times 3$  and  $6 \times 6$  MIMO channels in Case 2. Average receive SNR = 20 dB. (a) The receiver moves along the LOS street  $R_2$ . (b) The receiver moves along the NLOS street  $R_1$ .

- [9] C. B. Dietrich, K. Dietze, J. R. Nealy, and W. L. Stutzman, "Spatial polarization, and pattern diversity for wireless handheld terminals," *IEEE Trans. Antennas Propagat.*, vol. 49, no. 9, pp. 1271–1281, Sept. 2001.
- [10] M. R. Andrews, P. P. Mitra, and R. deCarvalho, "Tripling the capacity of wireless communications using electromagnetic polarization," *Nature*, vol. 409, pp. 316–318, Jan. 2001.
- [11] L. Dong, R. W. Heath, and H. Ling, "MIMO wireless handheld terminals using antenna pattern diversity," *submitted to IEEE Trans. Wireless Commun.*, June 2002.
- [12] P. F. Driessen and G. J. Foschini, "On the capacity formula for multiple input multiple output wireless channels: A geometric interpretation," *IEEE Trans. Commun.*, vol. 47, no. 2, pp. 173–176, Feb. 1999.
- [13] W. C. Jakes, *Microwave Mobile Communications*, John Wiley and Sons, New York, 1974.
- [14] J. Perez, F. Saez de Adana, O. Gutierrez, I. Gonzalez, F. Catedra, I. Montiel, and J. Guzman, "FASANT: fast computer tool for the analysis of on-board antennas," *IEEE Antenna Propagat. Mag.*, vol. 41, pp. 84–98, Apr. 1999.